Mechanism of the Forbidden [3s,5s]-Sigmatropic Shift: Orbital Symmetry Influences Stepwise Mechanisms Involving Diradical Intermediates

Andrew G. Leach, Saron Catak, and K. N. Houk*[a]

Abstract: The mechanisms of [3s,5s]-sigmatropic shifts of octa-1,3,7-triene and 7-methylenenona-1,3,8-triene have been elaborated using B3LYP and BPW91 density functional theory and CASPT2 methods. These orbital symmetry forbidden rearrangements are stepwise, involving diradical intermediates. A comparison with several [3,3]-sigmatropic shifts of substituted hexadienes and of [5,5]-sigmatropic shifts that are allowed, but nevertheless follow stepwise paths, shows that the activation barrier for the disallowed [3,5] shift is significantly larger than that for the stepwise reactions that are orbital symmetry allowed. Cyclic diradicals that have an aromatic circuit of electrons including the two radical centers and conjugated π or σ bonds are stabilized as compared to cyclic diradicals with an antiaromatic circuit of electrons. This applies to the transition states leading to and from the diradicals and influences the activation energies of stepwise sigmatropic shifts. The magnitudes of these effects are small but will have a significant influence on the rates of competing processes. This series of calculations has been used to assess the relative capabilities of the two functionals. We find that BPW91 underestimates the endothermicity of diradical formation and the barrier to diradical formation whereas B3LYP overestimates these quantities.

Keywords: ab initio calculations · density functional calculations · diradical intermediate · reaction mechanism · sigmatropic rearrangement

Introduction

The orbital symmetry selection rules proposed by Woodward and Hoffmann establish those pericyclic reactions that may occur by concerted pathways.[1] An "allowed" reaction maintains bonding interactions in the cyclic transition state of the concerted reaction. A useful formulation of these rules states that concerted transition states of allowed pericyclic reactions are aromatic, while the hypothetical transition states of forbidden concerted reactions are antiaromatic.[2, 3] Such forbidden processes must occur by lower energy stepwise paths involving diradical intermediates.

Stepwise reaction mechanisms also occur for some orbital symmetry allowed processes; radical stabilizing substituents can cause diradical intermediates to be more stable than concerted transition states. Indeed, much mechanistic attention of the late twentieth century was focussed upon whether allowed reactions occur by concerted or stepwise mechanisms.[4] Interest in this question has not entirely subsided.[5]

Classically, the feasibility of a stepwise path has been established by thermochemical estimates.[6, 7] For example, the energy of cyclohexan-1,4-diyl, **2**, a potential intermediate in the Cope rearrangement of 1,5-hexadiene, **1**, has been estimated from twice the CH bond dissociation energy of cyclohexane (Scheme 1).[8] This bond dissociation energy is taken as equal to that for propane forming a propyl radical—no interaction between the two radical centers is assumed, in spite of well-established through-σ-bond coupling of radical centers.[9]

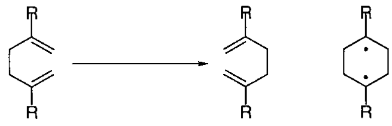

1 **2**

	R
a	H
b	vinyl
c	phenyl

Scheme 1. Several [3,3]-sigmatropic shifts (Cope rearrangements) and a potential diradical intermediate, **2**.

The [3s,5s]-sigmatropic shift is an example of an orbital-symmetry forbidden reaction that must occur by a stepwise

---

[a] Prof. Dr. K. N. Houk, Dr. A. G. Leach, S. Catak
Department of Chemistry and Biochemistry
University of California
Los Angeles, CA 90095-1569 (USA)
Fax: (+1)310-206-1843
E-mail: houk@chem.ucla.edu

0947-6539/02/0806-1290 $ 17.50+.50/0

pathway involving a diradical intermediate. We have explored several examples of this reaction with quantum mechanical methods. These studies show that orbital symmetries influence significantly the activation energies of stepwise reactions involving diradical intermediates and transition states. The energetic consequences are modest, but sufficiently large to influence the rates and product distributions of reactions involving diradical intermediates. These results, along with evidence from studies of forbidden [2 + 2] cycloadditions[10] and 1,3-shifts,[11] show that vestiges of the orbital symmetry control that has such a powerful influence on concerted reactions appear even in stepwise reactions involving diradical intermediates.

Background

Suprafacial sigmatropic shifts are thermally allowed for $4n+2$ electron systems. Thus, [3s,3s]- and [5s,5s]-sigmatropic shifts are allowed, while the [3s,5s] is forbidden. After decades of debate, evidence has settled on the concerted mechanism for the parent Cope rearrangement of **1a**.[4] The preference for concert can be overcome, however, by appropriate substitution. When highly radical stabilizing 2- and 5-substituents are present (e.g., **1b** or **1c**) stepwise mechanisms involving stabilized diradical intermediates, **2**, become favored over concerted.[12]

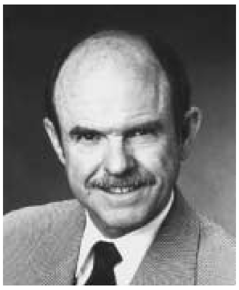

Editorial Board Member:[*] *K. N. Houk received his undergraduate and graduate degrees at Harvard, working with Professor R. B. Woodward as a graduate student in the area of experimental tests of orbital symmetry selection rules. He has been on the faculties of Louisiana State University, the University of Pittsburgh, and UCLA. Professor Houk received the LSU Distinguised Research Master Award in 1978, the von Humboldt U.S. Senior Scientist Award in 1981, and an Arthur C. Cope Scholar Award from the American Chemical Society in 1988. He was the 1991 recipient of the ACS James Flack Norris Award in Physical Organic Chemistry and 1998 winner of the Schrödinger Medal of the World Association of Theoretically Oriented Chemists (WATOC). He received the Bruylants Chair from the University of Louvain-la-Neuve in Belgium in 1998 and an honorary doctorate (Dr.rer.nat.h.c.) from the University of Essen in Germany in 1999. He won the Tolman Medal of the Southern California Section of the American Chemical Society in 1999. From 1988–1990, he was Director of the Chemistry Divison of the National Science Foundation. He was Chairman of the UCLA Department of Chemistry and Biochemistry from 1991–1994. He is Fellow of the AAAS and of the WATOC, and was an Erskine Fellow in New Zealand, a Lady Davis Fellow in Israel, and a JSPS Fellow in Japan. Professor Houk is an authority on theoretical organic chemistry, and his group is involved in developments of rules to understand reactivity and selectivity, computer modeling of organic and biochemical reactions, and experimental tests of the predictions of theory. He has published over 500 articles in refereed journals and is one of the top cited chemists of the last two decades.*

Although thermally allowed, the [5,5]-sigmatropic shift of **3** is also predicted theoretically to be stepwise (Scheme 2).[13] This is a consequence of the bis-allylic stabilization of the intermediate **4**. The transition state linking this diradical to **3** is predicted to be more stable than a concerted transition state.

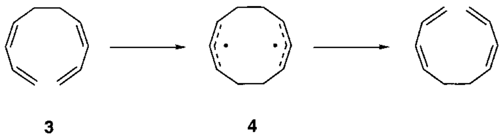

Scheme 2. The stepwise mechanism of the [5,5]-sigmatropic shift.

The [3s,5s]-sigmatropic shift is a forbidden process, and is expected to occur, if at all, through a stepwise process. The hydrocarbon [3s,5s]-sigmatropic shift of trienes such as **5** is so far unknown, although a heterocyclic, photochemical [3,5] shift has found synthetic utility (Scheme 4).[14] Birney et al. have found that formal [3,5]-sigmatropic shifts of several dienyl esters (Scheme 5) are actually pseudopericyclic processes, not involving a cyclic delocalized system and not subject to the Woodward–Hoffmann rules.[15] Such processes are facilitated by the involvement of lone pairs in orbitals orthogonal to the π-system. These lone pairs are absent in the all-hydrocarbon process, and a pseudopericyclic process is not possible. Miller has explored the rearrangements of cyclohexadienes.[16] He found that one of the products of an acid-catalyzed rearrangement of a crotyl substituted cyclohexadiene arises from a formal [3,5]-sigmatropic shift (see Scheme 6) but attributed this to two successive Wagner–Meerwein migrations followed by a Cope rearrangement.[17]

The [3,5]- and [5,5]-sigmatropic shifts of the parent systems cannot be detected experimentally, and 1,3,7-octatriene (**5a**) and 1,3,7,9-decatetraene (**3**) can undergo alternative Cope rearrangements (see Scheme 3). Thus, **5a** undergoes a Cope rearrangement forming **7** with an activation enthalpy of 38.0 kcal mol^{-1}.[18]

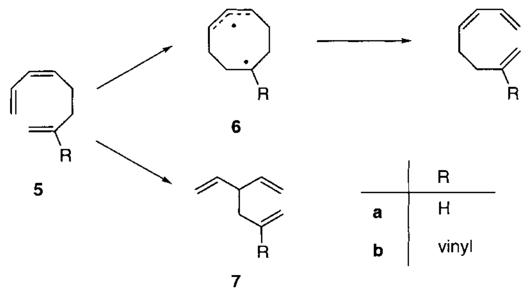

Scheme 3. The stepwise [3,5]-sigmatropic shift and the product of a competing [3,3]-sigmatropic shift.

Against this setting, we have explored the parent hydrocarbon [3s,5s] shift and have revisited the corresponding parent [3,3] and [5,5] shifts theoretically. B3LYP is known to accurately reproduce experimental activation energies and

---

[*] Members of the Editorial Board will be introduced to readers with their first manuscript.

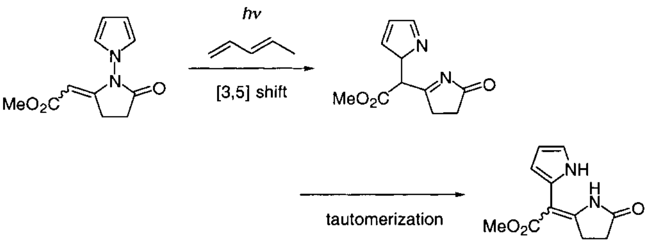

Scheme 4. A photochemically mediated [3,5]-sigmatropic shift, employed in the synthesis of tetrapyrroles.[14]

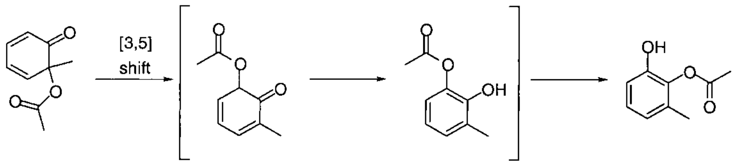

Scheme 5. The [3,5]-sigmatropic shift of a dienyl ester predicted to follow a pseudo-pericyclic mechanism.[15]

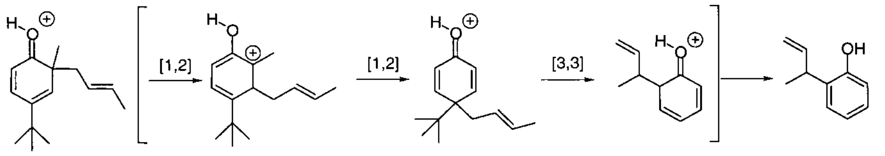

Scheme 6. The acid catalyzed formal [3,5]-sigmatropic shift of a crotyl-substituted cyclohexadiene has been explained by two [1,2]-Wagner–Meerwein shifts followed by a [3,3]-Cope rearrangement.[17]

energies of pericyclic reactions, including concerted and stepwise mechanisms.[19] Some doubt has recently been cast on its ability to describe some singlet diradicals.[20] In a report on the [3,3] shifts of 1,5-hexadiene and some cyano-substituted analogues, BPW91 was advocated by Staroverov and Davidson as a better functional for such systems; second-order perturbation theory corrected CASSCF (MROPT2) energies were used as the standard against which the functionals may be assessed.[21] Our calculations employed the B3LYP and BPW91 functionals for geometry optimizations, and CASPT2 single point calculations using the B3LYP geometries provided a standard against which these functionals were tested.

Thermochemical estimates were also made of the energies of the cyclic diradical intermediates involved in stepwise paths. Such energies account for the strain inherent in these cyclic structures but take no account of any non-classical electronic effects. The transition states and intermediates were further characterized by evaluation of the nucleus independent chemical shift (NICS) value at the center of each ring. This provides a measure of the change of magnetic susceptibility and has been used to differentiate aromatic and antiaromatic systems.[22]

Computational Methods

B3LYP and BPW91 calculations were performed in Gaussian98.[23] Diradicals and transition states leading to diradicals were treated with unrestricted B3LYP and BPW91; HOMO–LUMO mixing in the initial guess led to unrestricted wave functions when these were more stable than restricted wave functions. Diradical wave functions are not spin eigenfunctions and are generally spin-contaminated. $\langle S^2 \rangle$ values provide an indication of the degree of contamination of the singlet diradical wave function by triplet states and those of even higher multiplicity. All minima and transition states were characterized by their vibrational frequencies, and all reported energetics include unscaled zero-point and thermal corrections to 298 K.

CASPT2 single point calculations were performed in MOLCAS5 and utilized the B3LYP geometries.[24] The CASPT2 calculations apply a second-order perturbation correction to CASSCF calculations. The CASSCF calculations used an active space consisting of six electrons in six orbitals for the [3,3] shift of **1a**, eight electrons in eight orbitals for the [3,5] shift of **5a** and ten electrons in ten orbitals for the [3,3] shift of **1b**, the [3,5] shift of **5b** and the [5,5] shift of **3**. The active space orbitals were chosen to correspond to the σ bonding orbital of the σ bond in the reactant that is ultimately broken in the sigmatropic shift and all of the π bonding orbitals of the reactant and the antibonding counterparts of each of these orbitals. The B3LYP zero-point and thermal corrections were applied to these CASPT2 single point energies without scaling. B3LYP, BPW91 and CASPT2 calculations all employed the 6-31G* basis set. Spin projection was performed based on the reported values of $\langle S^2 \rangle$ for contaminated singlets and the energies and values of $\langle S^2 \rangle$ for triplet single points at the same geometry. A method analogous to that reported for UHF was employed.[25]

Two thermochemical estimates of the energies of cyclic diradicals were made, one using empirical data and the other using the MM2 force field[26] in MacroModel 7.[27] Benson's thermochemical tables were used to calculate the enthalpy of formation of carbocycles corresponding to the addition of two H atoms to various cyclic diradical intermediates.[6] The bond dissociation energy (BDE) for each of the two CH bonds formed by this addition of H atoms was estimated using empirical data assembled by Roth et al.[18] The addition of these BDEs to the enthalpy of formation of the carbocycle provides an estimate of the enthalpy of formation of each cyclic diradical. The enthalpies of formation of the reactant polyenes were also estimated using Benson's tables and used to predict an empirical enthalpy change for the formation of cyclic diradicals.

NICS values were calculated by defining a ghost atom at the center of the ring in each cyclic transition state and diradical. Application of the NMR keyword in Gaussian98 in combination with the UB3LYP/6-31G* or UBPW91/6-31G* method generated isotropic chemical shifts for the ghost atom.

Results and Discussion

Calculated energetics: We explored the potential energy surface of the [3,5]-sigmatropic shift of octa-1,3,7-triene (**5a**) at both B3LYP/6-31G* and BPW91/6-31G* levels. We were unable to find a concerted transition state but instead located a diradical intermediate **6a** and a transition structure, **8a**, linking it to reactants. CASPT2/6-31G* single point calculations were performed on the B3LYP/6-31G* geometries.

Figure 1 shows the UB3LYP/6-31G* geometries for the transition state **8a** and intermediate **6a** for the stepwise [3,5] shift, of octa-1,3,7-triene. The activation enthalpy and enthalpy change on formation of the diradical intermediate at the three levels of theory are reported below the structures. While the three levels agree well on the energy of the diradical, B3LYP places the transition structure, **8a**, 4 kcal mol^{-1} higher in energy than the other two methods. This is related to the greater spin contamination in the B3LYP transition structure. Both B3LYP and BPW91 predict that $\langle S^2 \rangle = 1.03$ for the diradical intermediate, which indicates that the diradical is nearly 50:50 singlet and triplet, and the singlet and triplet are nearly degenerate. B3LYP predicts $\langle S^2 \rangle = 0.66$ and BPW91 predicts $\langle S^2 \rangle = 0.50$ for the transition state leading to the diradical. This indicates contamination with the higher energy triplet (and other higher multiplicity states). This increases the energy of the spin-contaminated state. The UB3LYP case has more contamination, and this will raise the energy of the transition structure. Spin projection using the value of $\langle S^2 \rangle$ for the contaminated singlet and the $\langle S^2 \rangle$ value and energy from a triplet single point at the singlet geometry[25] lowers $\Delta H^{\neq}$ to 37.8 kcal mol^{-1} for B3LYP and to 35.3 kcal mol^{-1} for BPW91. ΔH_{int} is little changed after spin projection, with corrections of -0.1 kcal mol^{-1} calculated for both functionals.

Most allowed hydrocarbon pericyclic reactions have been observed to have an activation barrier of approximately 34 kcal mol^{-1}. This [3,5]-sigmatropic shift has a barrier higher than this by 5–7 kcal mol^{-1}. The diradical is found to be lower in energy than the transition state leading to it or away from it by anywhere from 4–7 kcal mol^{-1}.

In the transition structure, **8a**, the length of the breaking bond is virtually unchanged from that in the reactant. The bond is 1.549 Å (B3LYP) or 1.555 Å (BPW91) long in the reactant compared with 1.556 Å or 1.555 Å in transition structure **8a**. In the diradical intermediate, **6a**, both the "breaking" and "forming" bonds are elongated by 0.02–0.03 Å compared with the unperturbed CC σ bond length in the reactant.

B3LYP/6-31G* calculations predict that the known [3,3]-sigmatropic shift of **5a** which forms **7** is concerted, passing through transition state **16**, with an activation enthalpy of 37.9 kcal mol^{-1}, in good agreement with the experimentally determined value of 38.0 kcal mol^{-1},[18] and 1–5 kcal mol^{-1} below the activation energy computed for the stepwise [3,5] shift. It is interesting that the activation energy for the [3,3] shift is about 4 kcal mol^{-1} higher than that of the parent system (**1a**). The vinyl substituent stabilizes the reactant, **5a**, and also must assume an axial position in the transition state, **16**, of the Cope rearrangement (Figure 1).

To make comparisons to allowed shifts, we have also obtained the previously reported B3LYP/6-31G* transition states and intermediates for the [3,3] shift of **1a** and the [5,5] shift of **3**.[12, 13] These were reoptimized with UBPW91/6-31G* and were also used as geometries for CASPT2/6-31G* single points such that all cases have comparable data.

Figure 2 shows the concerted transition structure of the allowed [3,3] shift of **1a** according to B3LYP and BPW91. The enthalpy of activation for this parent Cope rearrangement has been measured experimentally to be 33.5 ± 0.5 kcal mol^{-1}.[7]

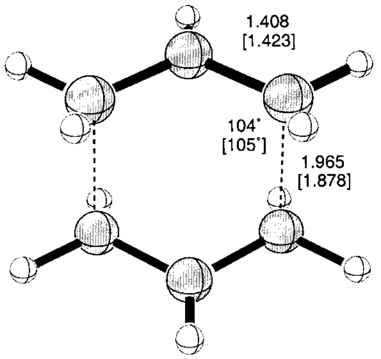

9a

	$\Delta H^{\neq}$
B3LYP:	33.2
BPW91:	26.7
CASPT2:	32.3

Figure 2. The concerted transition state, **9a**, for the [3,3]-sigmatropic shift of 1,5-hexadiene. The structure shown was obtained with B3LYP/6-31G*. Distances [Å] and angles are reported for the B3LYP geometry with the corresponding values for the BPW91 geometry in brackets. Enthalpies at 298 K relative to 1,5-hexadiene are reported in kcal mol^{-1}.

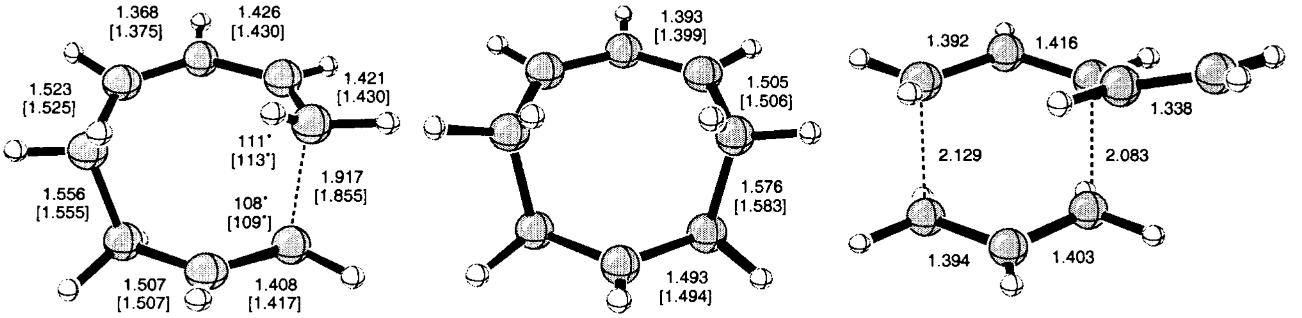

	8a	**6a**	**16**
	$\Delta H^{\neq}$	ΔH_{int}	$\Delta H^{\neq}$
B3LYP:	42.9 (37.8)	35.8 (35.7)	37.9
BPW91:	38.5 (35.3)	34.4 (34.3)	
CASPT2:	38.9	34.4	

Figure 1. The transition state, **8a**, and diradical intermediate, **6a**, for the [3,5]-sigmatropic shift of 1,3,7-octatriene, **5a**, and the transition state, **16**, for a competing Cope rearrangement. The structures shown were obtained with UB3LYP/6-31G*. Distances [Å] and angles are reported for the UB3LYP geometries with the corresponding values for the UBPW91 geometries in brackets. Enthalpies at 298 K relative to **5a** are reported in kcal mol^{-1}. Values in parentheses were obtained by projecting out the triplet spin contamination.

The B3LYP and CASPT2 energetics are in good agreement with this while BPW91 underestimates the barrier by 7 kcal mol^{-1}. The activation enthalpy is calculated to be 7–12 kcal mol^{-1} lower than for the forbidden [3,5] shift of **5a**.

Various calculations give the partial bond length as 1.9–2.0 Å, although the energy is not very sensitive to the distance.[4b, 28] Correlating theoretically predicted kinetic isotope effects with experimentally observed values predicts a partial bond length in the "real" transition structure of 2.085 Å, closer to the B3LYP value of 1.965 Å than the BPW91 value of 1.878 Å.[28]

It was previously reported that no concerted transition state could be found using B3LYP/6-31G* for the allowed [5,5] shift of **3**. We have found that this is also the case with BPW91/6-31G*. The diradical **4** and transition state **10** linking it to reactants could be located at both levels of theory and are shown in Figure 3. Both functionals are in reasonable agreement concerning the energy of diradical **4**. The elevated energy of this diradical predicted by UB3LYP corresponds to a larger degree of spin contamination in the UB3LYP structure ($\langle S^2 \rangle = 0.92$) compared with the UBPW91 structure ($\langle S^2 \rangle = 0.51$). The two functionals make predictions of the activation enthalpy that differ by 7.2 kcal mol^{-1}. BPW91 predicts a barrier 4 kcal mol^{-1} lower than CASPT2 and B3LYP predicts a barrier that is 3.2 kcal mol^{-1} higher. This mirrors the different degree of spin contamination in the two transition structures. Spin projection lowers $\Delta H^{\neq}$ to 30.3 for B3LYP but makes negligible change to the BPW91 energy. The activation energies for this [5,5] shift are calculated to be 9–13 kcal mol^{-1} lower than for the [3,5] shift of **5a** and lower by up to 3 kcal mol^{-1} than for the [3,3] shift of **1a**. The diradical is found to be in a well of depth 1–6 kcal mol^{-1}.

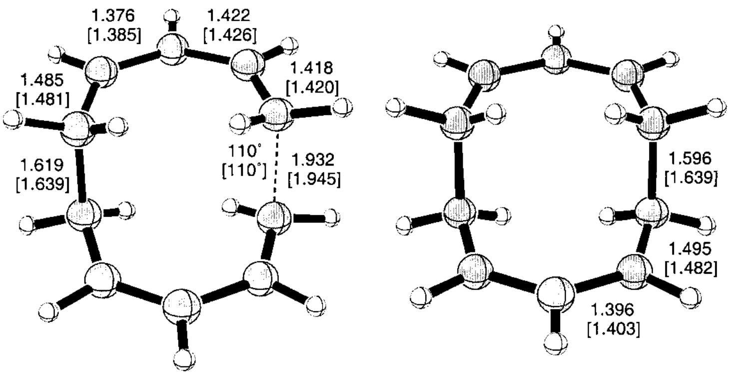

10 **4**

	$\Delta H^{\ddagger}$		ΔH_{int}
B3LYP:	32.9 (30.3)	B3LYP:	27.1 (24.4)
BPW91:	25.7 (25.7)	BPW91:	24.4 (21.6)
CASPT2:	29.7	CASPT2:	23.8

Figure 3. The transition state, **10**, and diradical intermediate, **4**, for the [5,5]-sigmatropic shift of 1,3,7,9-decatetraene, **3**. The structures shown were obtained with UB3LYP/6-31G*. Distances [Å] and angles are reported for the UB3LYP geometries with the corresponding values for the UBPW91 geometries in brackets. Enthalpies at 298 K relative to **3** are reported in kcal mol^{-1}. Values in parentheses were obtained by projecting out the triplet spin contamination.

The breaking bond in transition structure **10** is stretched compared with the same bond in the reactant tetraene, **3**, by 0.07–0.08 Å (from 1.552 Å with B3LYP and 1.558 Å with BPW91). The forming bond is also long (1.93–1.95 Å) in this transition state—BPW91 even predicts that it is longer than its counterpart distance (1.88 Å) in the concerted [3,3]-transition state **9a**, discussed above. The corresponding distances in the diradical **4** (1.596 Å with B3LYP or 1.639 Å with BPW91) are remarkably long for what is formally a normal C–C single bond. It should be noted that the breaking and the forming σ bonds are both longer in **10** and **4** than in their [3,5] counterparts **8a** and **6a**.

The data for the parent hydrocarbon [3,3], [3,5] and [5,5] shifts presented above suggests that the barrier to the two allowed reactions is considerably lower than that for the forbidden [3,5] shift, even when the [5,5] process involves a stepwise mechanism. However, these three examples are not readily comparable as their differing atomic constitutions may be responsible for the differences. In particular, **4** is a doubly allylically stabilized diradical, while **6a** is composed of an allylic and a secondary radical.

To provide a direct comparison of systems with nominally equal intermediate energy, a set of three isomeric decatetraenes, **1b**, **5b** and **3**, was studied (Figure 4). These three molecules can undergo a [3,3]-, a [3,5]- and a [5,5]-sigmatropic shift, each of which follows a stepwise path and each of which involves a diradical intermediate composed of two allylic radicals. More meaningful comparisons of activation energies and intermediate geometries may be made between these reactions.

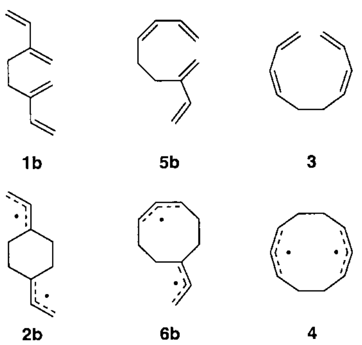

Figure 4. Isomeric decatetraenes which can undergo [3,3]- (**1b**), [3,5]- (**5b**) or [5,5]- (**3**) sigmatropic shifts. These reactions may all involve isomeric diradicals **2b**, **6b**, or **4**.

Figure 5 shows the calculated structures of the diradical intermediates and transition structures for the stepwise sigmatropic shifts of **1b**, **5b**, and **3**. Both B3LYP/6-31G* and BPW91/6-31G* calculations predict that the [3,3] shift of **1b**, the [3,5] shift of **5b** and the [5,5] shift of **3** all proceed through stepwise paths, and no concerted transition states could be found even with restricted calculations.

As observed with the parent shifts already discussed, it can be seen that B3LYP predicts ΔH_{int} values that are higher than CASPT2 standard values by 1–3 kcal mol^{-1}. B3LYP activation barriers are too high by 3–4 kcal mol^{-1}. On the other hand, BPW91 predicts ΔH_{int} values that are about correct for

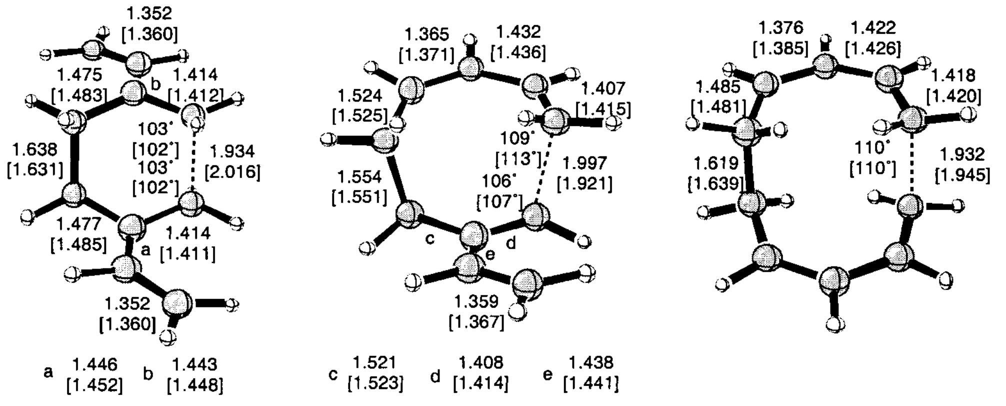

	11b	8b	10
	$\Delta H^{\ddagger}$	$\Delta H^{\ddagger}$	$\Delta H^{\ddagger}$
B3LYP:	24.2 (23.1)	37.3 (32.8)	32.9 (30.3)
BPW91:	16.8 (16.8)	32.2 (30.7)	25.7 (25.7)
CASPT2:	20.1	33.6	29.7

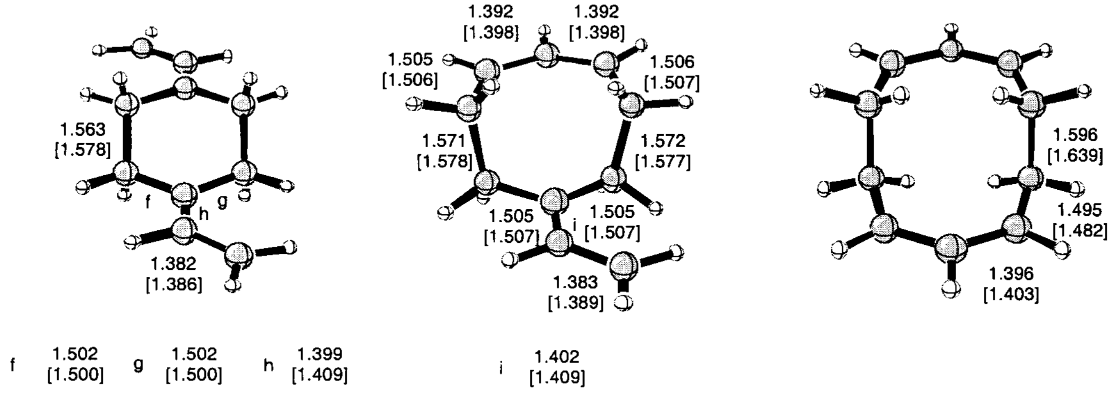

	2b	6b	4
	ΔH_{int}	ΔH_{int}	ΔH_{int}
B3LYP:	13.9 (12.7)	29.2 (29.2)	27.1 (30.3)
BPW91:	11.5 (9.7)	23.3 (23.3)	24.4 (21.6)
CASPT2:	12.6	27.6	23.8

Figure 5. The transition states and intermediates for the [3,3] shift of **1b**, the [3,5] shift of **5b** and the [5,5] shift of **3**. The geometries shown were obtained with UB3LYP/6-31G*. Distances [Å] and angles are reported for the B3LYP geometries with the corresponding values for the BPW91 geometry reported underneath in brackets. Enthalpies, at 298 K, are reported relative to the appropriate reactant tetraene in kcal mol^{-1}. Values in parentheses were obtained by projecting out the triplet spin contamination.

the [3,3] and [5,5] shifts but too low by 4 kcal mol^{-1} for the [3,5] shift. BPW91 activation barriers are underestimated by 1–4 kcal mol^{-1}. As with the parent hydrocarbon shifts, this discrepancy correlates with the degree of spin contamination for each structure and spin projection using the reported values of $\langle S^2 \rangle$ improve the B3LYP energies compared to CASPT2 but reduce agreement for BPW91.

The activation enthalpy for the stepwise mechanism of the forbidden [3,5] shift of **5b** is calculated to be 13–15 kcal mol^{-1} higher than for the [3,3] shift of **1b** and 4–7 kcal mol^{-1} higher than for the [5,5] shift of **3**. The [3,3]-diradical **2b** is bound by 5–10 kcal mol^{-1}, the [3,5]-diradical **6b** by 6–9 kcal mol^{-1} and the [5,5]-diradical **4** by 1–6 kcal mol^{-1}.

The two functionals differ in their predictions of the length of the forming bond in the transition structures. BPW91 predicts that the [3,5]-transition structure **8b** has the shortest forming bond (1.921 Å compared with 2.016 Å for **11b** and 1.945 Å for **10**). B3LYP predicts the reverse with the [3,5] transition structure **8b** having the longest forming bond length (1.997 Å). Both functionals predict that the breaking bond is stretched to 1.61–1.64 Å (from 1.55–1.56 Å in the reactant tetraenes **1b** and **3**) in the [3,3]- and [5,5]-transition states **11b** and **10**. This compares to a barely perturbed bond in the [3,5]-transition structure **8b** (1.55 Å compared with 1.55–1.56 Å in reactant **5b**).

The diradicals **2b**, **6b** and **4** are also shown in Figure 5. The energy change on formation of the diradical is higher for the

[3,5] and [5,5] shifts of **5b** and **3** (by 11 – 13 kcal mol^{-1}) than for the [3,3] shift of **1b**. The "breaking" and "forming" σ bond lengths are shorter in the [3,3] and [5,5] diradicals **2b** and **4** than in the transition states leading to them, **11b** and **10**. In contrast, the breaking bond stretches slightly from 1.55 to 1.57 Å on going from the [3,5]-transition state **8b** to the diradical **6b** while the forming bond contracts from > 1.9 Å to 1.57 Å. Each diradical is composed of two allylic radicals which enforce rigid, strained structures.

Diradicals **2b**, **6b** and **4** are all isomers and therefore, their absolute energies, calculated with our three chosen levels of theory may be compared. The six-membered ring diradical **2b** is lowest in energy. Eight-membered ring diradical **6b** is calculated to be 11 – 16 kcal mol^{-1} higher in energy. The ten-membered ring diradical, **4**, is 11 – 13 kcal mol^{-1} above **2b**. Transition states leading to and from the diradicals follow the same pattern.

The geometries and energies suggest that the diradical for the [3,5] shift, **6b**, is destabilized relative to **2b** and **4**. To investigate whether this difference is due to electronic effects that stabilize **2b** and **4** or just to differences in strain energy between these diradicals in different rings, we have also made thermochemical estimates of the diradical energies from hydrocarbon energies and bond dissociation energies.

Chemically similar isomers are good candidates for comparison by thermochemical and force field methods. The relative energies of the cyclic diradicals after optimization using the MM2 force field suggests that the eight-membered ring diradical, **6b**, should be 8 kcal mol^{-1} above its six-membered counterpart, **2b**. The ten-membered ring diradical, **4**, should be highest in energy and 10 kcal mol^{-1} above **2b**.

Estimates of the enthalpies of formation of the diradicals were also made using Benson's thermochemical tables[6] and Roth's CH bond dissociation energies.[18] Benson's tables were used to estimate the enthalpies of formation of 1,4-divinylcyclohexane and 5-vinylcyclooctene, corresponding to dihydro **2b** and **6b**, respectively. The enthalpy of formation of the corresponding structure for **4** (*cis,cis*-cyclodeca-1,6-diene) has been estimated elsewhere.[29] The dissociation energies for the two CH bonds cleaved to form **2b**, **6b** and **4** from these alkenes were estimated from the data assembled by Roth et al. for similar CH bonds.[30] The addition of the two bond dissociation energies to the enthalpies of formation of the cyclic diene yielded an estimate of the enthalpy of formation of the cyclic diradical. These showed that the six-membered ring diradical **2b** should be lowest in energy. Eight-membered ring diradical **6b** should be 9 kcal mol^{-1} higher in energy and ten-membered ring **4** should be 10 kcal mol^{-1} above **2b**.

Although the empirical energies are only accurate to within a few kcal mol^{-1}, they clearly show that strain plays an important part in determining the relative energy of cyclic diradicals. Strain alone does not account for all of the differences in energy between cyclic diradicals: We find that the quantum mechanical energies predict that the [3,5]-diradical **6b** is higher in energy than the [3,3]-diradical **2b** by 2 – 8 kcal mol^{-1} more than accounted for by strain alone. The [5,5]-diradical **4** is 1 – 3 kcal mol^{-1} lower in energy than predicted empirically. There is a quantum mechanical effect that destabilizes **6b** relative to estimates based on non-interacting diradicals, and stabilizes **2b** and **4** relative to these non-interacting diradical models. This is consistent with some degree of cyclic delocalization, stabilizing when six or ten electrons are involved and destabilizing when eight electrons are present in the cycle.

Benson's tables were also used to predict the enthalpy of formation of the reactant tetraenes **1b**, **5b** and **3**. Combined with our estimates of the energies of cyclic diradicals, empirical predictions of the enthalpy change on reaction to form the diradical (ΔH_{int}) were made. These were 20.0 kcal mol^{-1} for the [3,3] shift of **1b**, 27.9 kcal mol^{-1} for the [3,5] shift of **5b** and 27.3 kcal mol^{-1} for the [5,5] shift of **3**. These numbers, along with those for the parent systems calculated in an analogous fashion,[31] may be compared with our CASPT2 quantum mechanical calculations (Figure 6). This reveals the action of a 7 – 8 kcal mol^{-1} stabilizing electronic interaction in the case of the [3,3]-diradical **2b**, a 3 – 5 kcal mol^{-1} stabilization of the [5,5]-diradical, **4**, and a 0 – 1 kcal mol^{-1} destabilization of the [3,5]-diradical, **6b**. The parent shifts are in line with this apart from the [3,5] diradical **6a** which is stabilized with CASPT2 compared to the empirical energy.

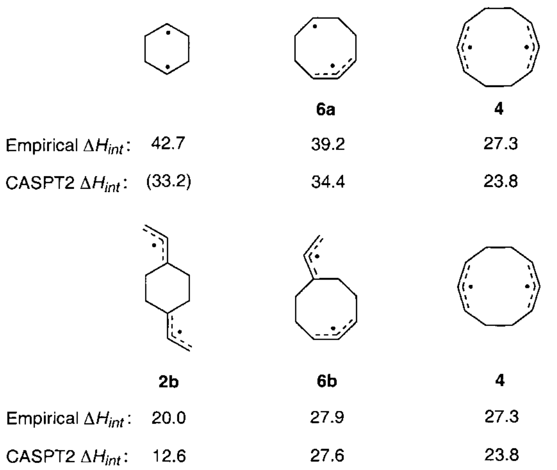

Figure 6. Enthalpy changes of cyclic diradical formation from reactant polyenes calculated by empirical methods and by CASPT2. The CASPT2 value for cyclohexan-1,4-diyl is actually for the concerted Cope transition state.

Cyclic delocalization: We have found that the barriers to the forbidden [3,5] shifts exceed those of allowed [3,3] and [5,5] shifts even when they take stepwise pathways. That this arises from cyclic delocalization is supported by the fact that in the stepwise transition structures for allowed reactions (**11b** and **10**), the breaking bond is considerably longer (1.62 – 1.64 Å) than in the comparable structures for forbidden [3,5] shifts, **8a** and **8b** (1.55 – 1.56 Å).

Strain may also play a part in determining these bond lengths by contributing to a lengthening in the [3,5] case to minimize the impact of partially eclipsed CH and CC bonds. The "forming" and "breaking" bonds are 1.56 – 1.58 Å in the [3,3]-diradical, **2b**, compared with 1.57 – 1.58 Å in the [3,5]-diradical, **6b**, and 1.60 – 1.64 Å in the [5,5]-diradical, **4**.

0947-6539/02/0806-1296 $ 17.50+.50/0

Cyclic delocalization by through-bond coupling is favored for $4n+2$ electrons but disfavored for $4n$ in these suprafacial geometries.[9, 33] We expect that this effect will be most pronounced when the diradicals have no exocyclic delocalization and consequently can only rely upon cyclic delocalization for stabilization. In accord with this, we find the most pronounced geometric variations for the three parent sigmatropic shifts of **1a**, **3** and **5a**.

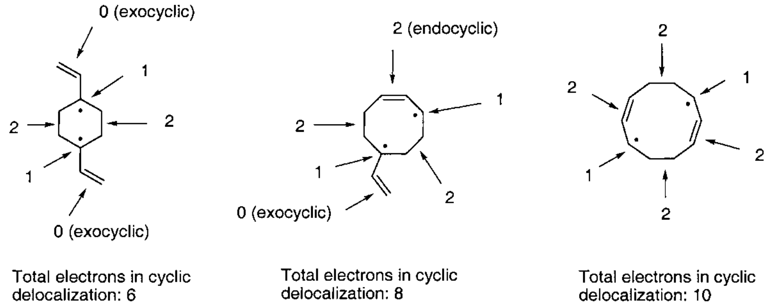

Figure 7. Electron counting for cyclic diradicals. The same principles apply to cyclic transition states linking to diradicals.

This cyclic delocalization and the aromatic or antiaromatic character it imparts, even to stepwise reactions, is also evidenced in the nucleus independent chemical shift (NICS) values, evaluated at the center of the ring in each transition state and intermediate. Negative values indicate aromatic and positive values antiaromatic character. It is found that benzene has a NICS value of around −13.[32a] The concerted transition state of the allowed parent Diels–Alder reaction between ethene and butadiene has a NICS value of about −19.[32] In accord with this, we find that the parent concerted Cope reaction has NICS values of −22.1 with B3LYP and −20.3 with BPW91. These values compare well with the values of −16 to −19 calculated by Schleyer et al. with different levels of calculations.[32] The allowed [5,5] shift of **3** has values of −6.5 (B3LYP) or −8.7 (BPW91) in the stepwise transition state, **10**, and −1.2 (B3LYP) or −5.0 (BPW91) in the diradical intermediate, **4**. The forbidden [3,5] shift of **5a** on the other hand has NICS values of +7.4 (B3LYP) or +7.0 (BPW91) in the transition state leading to diradical **6b** and +3.3 or +4.7 in the diradical itself.

The NICS values also confirm that exocyclic stabilization diminishes the effect of cyclic delocalization. The stepwise transition state for the [3,3] shift of **1b** has NICS values of −12.5 (B3LYP) and −12.1 (BPW91). The diradical **2b** has values of −1.0 (B3LYP) and −2.1 (BPW91). Furthermore, the [3,5] shift of vinyl-substituted **5b** has values of +7.1 (B3LYP) and +5.9 (BPW91) in the stepwise transition state **8b** and +2.1 (B3LYP) and +2.9 (BPW91) in the diradical **6b**. A plot of breaking bond length versus NICS value for the stepwise transition states and diradicals confirms a correlation between these two properties.

Geometric and magnetic shielding properties indicate that cyclic delocalization operates in these stepwise sigmatropic shifts even when they are stepwise. This imparts aromatic character to the transition states and diradical intermediates of formally allowed shifts and antiaromatic character to formally forbidden shifts. Although this coupling of diradical centers is evidenced in the [5,5]-transition structure, it has little, if any impact on the energetics of this shift. This decrease in impact of cyclic delocalization as the size of the system increases has been observed previously.[33]

For each of these cyclic diradicals, the number of electrons involved in cyclic delocalization consists of one for each radical center, two for each of the σ bonds connecting radical fragments and overlapping with the radical π orbitals and two for each of the endocyclic π-bonds involved in radical delocalization (Figure 7). Electrons from groups exocyclic to the ring are not counted in determining whether the system is aromatic or antiaromatic.

Generalizations and extensions

Orbital symmetry is well known to have a major influence on the activation energies of concerted pericyclic processes. This work establishes that orbital symmetry also influences stepwise mechanisms involving cyclic diradical intermediates. This conclusion should have application to other stepwise reactions which involve cyclic transition states. We highlight here two reported reactions whose product mixture is likely to have been influenced by the effects we have outlined.

For instance, the thermolysis of *trans*-1,2-divinylcyclobutane **12** is found to yield primarily (70%) the cyclohexene product **13**.[34] The *trans* ring junction disfavors concerted reactions, but the strained cyclobutane is readily thermolyzed to the diradical **14**. This diradical could plausibly combine in one of three ways—to regenerate the cyclobutane through a four-electron, four-membered transition state, to give the cyclohexene through a six-electron, six-membered transition state, or to give the cyclooctadiene **15** through an eight-electron eight-membered transition state (Scheme 7). The same preference for six electron cyclic transition states discussed above could contribute to the observed preference for **13**. This is a case where an acyclic, and therefore non-

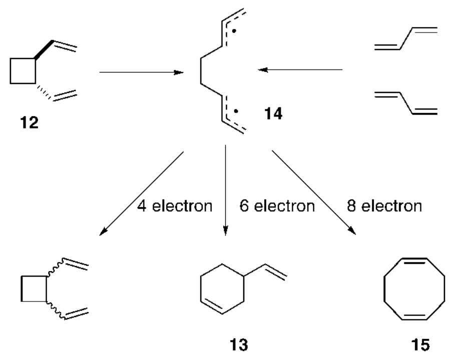

Scheme 7. Representative reactions which rates and product mixtures will be influenced by orbital symmetry even though they are not concerted. In these reactions, an acyclic diradical may cyclize through a number of competing cyclic transition states.

aromatic diradical, cyclizes through a cyclic transition state that can benefit from cyclic delocalization for $4n+2$ electrons but not $4n$.

A related case involves the dimerization of butadiene (and other dienes).[35] The principle product from such dimerizations is the cyclohexene Diels–Alder-type product (92%) which is believed to arise through both a stepwise mechanism involving the same diradical **14** discussed above and a competitive concerted mechanism.[36] Small amounts (8%) of the formal [2+2] product are also observed. An orbital symmetry preference for the six-electron cyclization leading to the cyclohexene product will influence this product mixture. Our earlier studies of this reaction predict little barrier to cyclization of diradical **14** via the six-membered ring, while the formation of the four-membered ring is disfavored.[37]

There is likely to be an orbital symmetry influence on the cyclization of diradicals in general. Doubleday found,[10] for example, that the tetramethylene diradical cyclizes by a pathway involving rotation of one methylene center (Figure 8), to endow the cyclization transition state with four-electron Möbius aromatic character.[3] We expect that all diradical cyclizations will occur preferentially by aromatic arrays rather than antiaromatic.

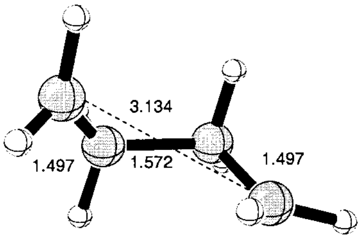

Figure 8. The favored CASSCF(4,4)/6-31G* transition state for the cyclization of the tetramethylene diradical, as reported by Doubleday. The transition state avoids a four-electron Hückel antiaromatic structure by twisting at one methylene terminus, endowing the structure with four-electron Möbius aromaticity.

Evaluation of functional performance

We observe that B3LYP predicts ΔH_{int} values that are higher than our CASPT2 estimates by 1–3 kcal mol^{-1}. B3LYP also predicts activation barriers for diradical formation that are 3–4 kcal mol^{-1} higher than CASPT2 values. By the same standard, BPW91 underestimates the endothermicity of the formation of the diradical (by up to 5 kcal mol^{-1}) and underestimates the activation barrier (by 0–4 kcal mol^{-1}). This difference in behavior of the functionals is mirrored in the values of $\langle S^2 \rangle$ which are all higher for UB3LYP than for UBPW91; this indicates greater contamination by higher multiplicity states in the UB3LYP wave function than in the UBPW91 wave function. Spin projection using the values of $\langle S^2 \rangle$ for the singlet and the triplet and triplet single point energies improves the B3LYP energetics, and the average signed error between B3LYP and CASPT2 reduces from +2.8 to +0.7 kcal mol^{-1}. On the other hand, the same procedure applied with BPW91 causes a reduction in agreement between this method and CASPT2 with the average signed error increasing from −1.7 to −2.9 kcal mol^{-1}. The utility of $\langle S^2 \rangle$ for evaluating the degree of spin contamination in unrestricted density functional methods has however been challenged and alternative methods may therefore be more appropriate when performing spin projection.[38]

The two functionals also differ in their prediction of geometries and NICS values. B3LYP predicts longer breaking bond lengths in the stepwise transition states than BPW91 but shorter corresponding lengths in the diradical intermediates than BPW91. With the exception of the transition state of the [5,5] shift, **10**, the NICS values are larger (either positive or negative) in the B3LYP transition states than in the BPW91 transition states but the reverse is true of diradical intermediates. These two observations are consistent with B3LYP incorporating more cyclic delocalization in the stepwise transition states than BPW91 but less in the intermediate diradicals.

Conclusion

The [3s,5s] rearrangement follows a stepwise path involving a diradical intermediate, but the activation barrier is significantly larger than the barrier for similar reactions which are allowed by the Woodward–Hoffmann rules even when they too follow stepwise paths. This vestige of forbiddenness disfavoring the stepwise [3,5]-sigmatropic shift even in a stepwise mechanism amounts to 2–5 kcal mol^{-1} and stems from cyclic delocalization in the transition state leading to the diradical intermediates. Consequently, orbital symmetry exerts a significant influence on the activation energies of potentially pericyclic sigmatropic shifts, even when they involve alternative stepwise mechanisms. The effect is large in the six-electron system and attenuates as the size of the system increases.

Acknowledgement

We are grateful to Professor David Birney for helpful discussions, the National Science Foundation for financial support, and Astra-Zeneca and the U.K. Fulbright Commission for a fellowship to A.G.L. We gratefully acknowledge grants of computer time from the UCLA Office of Academic Computing and the National Computational Science Alliance (under grant MCA93S015N, utilizing the NCSA HP/Convex Exemplar SPP-2000).

---

[1] R. B. Woodward, R. Hoffmann, *Angew. Chem.* **1969**, *81*, 797–869; *Angew. Chem. Int. Ed.* **1969**, *8*, 781–853; R. B. Woodward, R. Hoffmann, *The Conservation of Orbital Symmetry*, Verlag Chemie, Weinheim, **1970**.

[2] a) M. J. S. Dewar, *The Molecular Orbital Theory of Organic Chemistry*, McGraw-Hill, New York, **1969**, Chapter 8; b) M. G. Evans, *Faraday Soc. Trans.* **1939**, *35*, 824–834.

[3] H. E. Zimmerman, *Acc. Chem. Res.* **1971**, *4*, 272–280.

[4] a) K. N. Houk, J. González, Y. Li, *Acc. Chem. Res.* **1995**, *28*, 81–90; b) O. Wiest, D. C. Montiel, K. N. Houk, *J. Phys. Chem. A* **1997**, *101*, 8378–8388; c) W. T. Borden, *Mol. Phys.* **2002**, in press.

[5] a) W. v. E. Doering, J. L. Ekmanis, K. D. Belfield, F.-G. Klärner, B. Krawczyk, *J. Am. Chem. Soc.* **2001**, *123*, 5532–5541; b) D. A. Hrovat, W. T. Borden, *J. Am. Chem. Soc.* **2001**, *123*, 4069–4072.

[6] a) S. W. Benson, *Thermochemical Kinetics*, Wiley, New York, **1976**; b) S. W. Benson, F. R. Cruickshank, D. M. Golden, G. R. Haugen,

H. E. O'Neal, A. S. Rodgers, R. Shaw, R. Walsh, *Chem. Rev.* **1969**, *69*, 279–324.

[7] W. v. E. Doering, V. G. Toscano, G. H. Beasley, *Tetrahedron* **1971**, *27*, 5299–5306.

[8] W. v. E. Doering, Y. Wang, *J. Am. Chem. Soc.* **1999**, *121*, 10112–10118, and references therein.

[9] a) R. Hoffmann, A. Imamura, W. J. Hehre, *J. Am. Chem. Soc.* **1968**, *90*, 1499–1509; b) R. Hoffmann, *Acc. Chem. Res.* **1971**, *4*, 1–9; c) J. W. Verhoeven, *Recl. Trav. Chim. Pays-Bas* **1980**, *99*, 369–379.

[10] C. Doubleday, Jr., *J. Am. Chem. Soc.* **1993**, *115*, 11968–11983.

[11] a) S. Wilsey, K. N. Houk, A. H. Zewail, *J. Am. Chem. Soc.* **1999**, *121*, 5772–5786; b) K. N. Houk, M. Nendel, O. Wiest, J. W. Storer, *J. Am. Chem. Soc.* **1997**, *119*, 10545–10546; c) M. Nendel, D. Sperling, O. Wiest, K. N. Houk, *J. Org. Chem.* **2000**, *65*, 3259–3268; d) E. R. Davidson, J. J. Gajewski, *J. Am. Chem. Soc.* **1997**, *119*, 10543–10544.

[12] a) D. A. Hrovat, J. Chen, K. N. Houk, W. T. Borden, *J. Am. Chem. Soc.* **2000**, *122*, 7456–7460; b) D. A. Hrovat, B. R. Beno, H. Lange, H.-Y. Yoo, K. N. Houk, W. T. Borden, *J. Am. Chem. Soc.* **1999**, *121*, 10529–10537.

[13] B. R. Beno, J. Fennen, K. N. Houk, H. J. Lindner, K. Hafner, *J. Am. Chem. Soc.* **1998**, *120*, 10490–10493.

[14] P. A. Jacobi, S. C. Buddhu, D. Fry, S. Rajeswari, *J. Org. Chem.* **1997**, *62*, 2894–2906.

[15] a) D. M. Birney, X. Xu, S. Ham, *Angew. Chem.* **1999**, *111*, 147–150; *Angew. Chem. Int. Ed.* **1999**, *38*, 189–193; b) S. Quideau, M. A. Looney, L. Pouysegu, S. Ham, D. M. Birney, *Tetrahedron Lett.* **1999**, *40*, 615–618.

[16] B. Miller, *Acc. Chem. Res.* **1975**, *8*, 245–256.

[17] a) B. Miller, *J. Am. Chem. Soc.* **1969**, *91*, 2170–2172; b) B. Miller, *J. Am. Chem. Soc.* **1970**, *92*, 6246–6252.

[18] W. R. Roth, V. Staemmler, M. Neumann, C. Schmuck, *Liebigs Ann.* **1995**, 1061–1118.

[19] K. N. Houk, B. R. Beno, M. Nendel, K. Black, H.-Y. Yoo, S. Wilsey, J. K. Lee, *J. Mol. Struct. (THEOCHEM)* **1997**, *398–399*, 169–179.

[20] J. Gräfenstein, D. Cremer, *Phys. Chem. Chem. Phys.* **2000**, *2*, 2091–2103.

[21] V. N. Staroverov, E. R. Davidson, *J. Am. Chem. Soc.* **2000**, *122*, 7377–7385.

[22] a) P. v. R. Schleyer, C. Maerker, A. Dransfeld, H. Jiao, N. J. R. v. Eikema Hommes, *J. Am. Chem. Soc.* **1996**, *118*, 6317–6318; b) H. Jiao, R. Nagelkerke, H. A. Kurtz, R. V. Williams, W. T. Borden, P. v. R. Schleyer, *J. Am. Chem. Soc.* **1997**, *119*, 5921–5929; c) P. v. R. Schleyer (Editor), *Chem. Rev.* **2001**, *101*, 1115–1566.

[23] Gaussian 98 (Revision A.7), M. J. Frisch, G. W. Trucks, H. B. Schlegel, G. E. Scuseria, M. A. Robb, J. R. Cheeseman, V. G. Zakrzewski, J. A. Montgomery, R. E. Stratmann, J. C. Burant, S. Dapprich, J. M. Millam, A. D. Daniels, K. N. Kudin, M. C. Strain, O. Farkas, J. Tomasi, V. Barone, M. Cossi, R. Cammi, B. Mennucci, C. Pomelli, C. Adamo, S. Clifford, J. Ochterski, G. A. Petersson, P. Y. Ayala, Q. Cui, K. Morokuma, D. K. Malick, A. D. Rabuck, K. Raghavachari, J. B. Foresman, J. Cioslowski, J. V. Ortiz, B. B. Stefanov, G. Liu, A. Liashenko, P. Piskorz, I. Komaromi, R. Gomperts, R. L. Martin, D. J. Fox, T. Keith, M. A. Al-Laham, C. Y. Peng, A. Nanayakkara, C. Gonzalez, M. Challacombe, P. M. W. Gill, B. G. Johnson, W. Chen, M. W. Wong, J. L. Andres, M. Head-Gordon, E. S. Replogle, J. A. Pople, Gaussian, Inc., Pittsburgh PA (USA), **1998**.

[24] MOLCAS, Version 5, K. Andersson, M. Barysz, A. Bernhardsson, M. R. A. Blomberg, D. L. Cooper, T. Fleig, M. P. Fülscher, C. de Graaf, B. A. Hess, G. Karlström, R. Lindh, P.-Å. Malmqvist, P. Neogrády, J. Olsen, B. O. Roos, A. J. Sadlej, M. Schütz, B. Schimmelpfennig, L. Seijo, L. Serrano-Andrés, P. E. M. Siegbahn, J. Stålring, T. Thorsteinsson, V. Veryazov, P.-O. Widmark, Lund University (Sweden), **2000**.

[25] K. Yamaguchi, F. Jensen, A. Dorigo, K. N. Houk, *Chem. Phys. Lett.* **1988**, *149*, 537.

[26] N. L. Allinger, *J. Am. Chem. Soc.* **1977**, *99*, 8127–8134, and subsequent additions.

[27] MacroModel V7.0, copyright Columbia University 1986–1998, Schrodinger Inc. 1999: F. Mohamadi, N. G. J. Richards, W. C. Guida, R. Liskamp, M. Lipton, C. Caufield, G. Chang, T. Hendrickson, W. C. Still, *J. Comput. Chem.* **1990**, *11*, 440–467.

[28] O. Wiest, K. A. Black, K. N. Houk, *J. Am. Chem. Soc.* **1994**, *116*, 10336–10337.

[29] N. L. Allinger, J. T. Sprague, *J. Am. Chem. Soc.* **1972**, *94*, 5734–5747.

[30] The energy for CH cleavage to yield endocyclic allylic radicals (33.9 kcal mol^{-1}) was estimated from the BDE of *cis*-pent-2-ene (86.0 kcal mol^{-1}) and that for exocyclic allylic radicals (29.9 kcal mol^{-1}) from the BDE of 3-methylbut-1-ene (82.0 kcal mol^{-1}), ΔH_f(H atom) (52.1 kcal mol^{-1}) is subtracted from the BDE to arrive at the final value. These energy changes are then added to the enthalpies of formation of the diradical precursor.

[31] Enthalpies of formation of the reactant olefin and the dihydro adduct of each diradical were estimated from Benson's tables (ref. [6]). CH dissociation energies were estimated as described in footnote [30] with the addition of that for a non-conjugated secondary CH (e.g. a CH bond in cyclohexane). This latter was estimated as being the BDE of propane less ΔH_f(H atom), giving a value of 46.1 kcal mol^{-1}. Addition of two CH dissociation energies to the ΔH_f for the dihydro adduct enabled ΔH_f for the diradical and hence ΔH_{int} to be calculated.

[32] a) H. Jiao, P. v. R. Schleyer, *Angew. Chem.* **1995**, *107*, 329–332; *Angew. Chem. Int. Ed. Engl.* **1995**, *34*, 334–337; b) H. Jiao, P. v. R. Schleyer, *J. Phys. Org. Chem.* **1998**, *11*, 655–662.

[33] D. Sawicka, S. Wilsey, K. N. Houk, *J. Am. Chem. Soc.* **1999**, *121*, 864–865.

[34] a) J. A. Berson, P. B. Dervan, *J. Am. Chem. Soc.* **1973**, *95*, 267–270; b) V. Schüll, H. Hopf, *Tetrahedron Lett.* **1981**, *22*, 3439–3442.

[35] L. M. Stephenson, R. V. Gemmer, S. Current, *J. Am. Chem. Soc.* **1975**, *97*, 5909–5910.

[36] F.-G. Klärner, B. Krawczyk, V. Rusher, U. K. Deiters, *J. Am. Chem. Soc.* **1994**, *116*, 7646–7657.

[37] Y. Li, K. N. Houk, *J. Am. Chem. Soc.* **1993**, *115*, 7478–7485.

[38] a) V. N. Staroverov, E. R. Davidson, *J. Am. Chem. Soc.* **2000**, *122*, 186–187; b) E. Kraka, D. Cremer, *J. Comput. Chem.* **2001**, *22*, 216–229.

Received: October 5, 2001 [F3595]